

Magnetism and superconductivity of Fe/Nb/Fe trilayers

Th. Mühge, K. Westerholt, and H. Zabel

Institut für Experimentalphysik/Festkörperphysik, Ruhr-Universität Bochum, D-44780 Bochum, Germany

N. N. Garif'yanov, Yu. V. Goryunov, and I. A. Garifullin

Kazan Physicotechnical Institute of Russian Academy of Sciences, 420029 Kazan, Russian Federation

G. G. Khaliullin*

Max-Planck Institut für Festkörperforschung, D-70569 Stuttgart, Germany

(Received 23 August 1996; revised manuscript received 3 December 1996)

Sputtered Fe/Nb/Fe trilayers were prepared with Nb thicknesses d_{Nb} in the range 300–800 Å and with Fe thicknesses d_{Fe} in the range 0–30 Å. X-ray reflectivity measurements revealed the high quality of the film structure with low surface and interface roughnesses. Magnetic properties of the samples were studied using the magneto-optical Kerr effect, ferromagnetic-resonance and magnetization measurements by a SQUID magnetometer. For constant d_{Fe} a decrease of T_c with decreasing d_{Nb} was observed up to a critical thickness $d_{\text{Nb}}^{\text{crit}}$ below which superconductivity vanishes. We derived $d_{\text{Nb}}^{\text{crit}} \approx 320$ Å independent of d_{Fe} for $d_{\text{Fe}} \geq 7$ Å. The temperature dependence of the upper critical field $H_{c2}(T)$ showed two- and three-dimensional features for parallel and perpendicular orientations of the magnetic field, respectively. At the Nb/Fe interface in the trilayer systems an Fe-rich interlayer with nonmagnetic Fe is formed with a thickness depending sensitively on the preparation conditions. We observed a nonmonotonic dependence of the superconducting transition temperature T_c with increasing d_{Fe} and a definite maximum in $T_c(d_{\text{Fe}})$ at the onset of ferromagnetic order within the Fe layers. This maximum is attributed to a modification of the repulsive interaction between the electrons in the magnetically “dead” Fe-rich interlayer when an exchange field in the Fe layer is present.

[S0163-1829(97)02414-4]

I. INTRODUCTION

The interplay between superconductivity and ferromagnetism in dilute magnetic alloys and intermetallic compounds attracted considerable attention during the last 30 years (see, e.g., Ref. 1). The complex mutual influence of superconductivity and ferromagnetism may acquire new peculiarities in artificial systems like multilayers of superconducting-ferromagnetic (SC/FM) materials due to the proximity effect. Experimental investigations of the proximity effect in SC/FM layered systems were started by Hauser, Theurer, and Werthamer.² They studied the depression of the superconducting transition temperature T_c in the bilayered Pb/NM systems in which NM denotes various types of materials: ferromagnetic Fe, Ni, and Gd, antiferromagnetic Cr, and dilute magnetic alloys like 1 at. % Fe in Mo or 2.9 at. % Gd in Pb. The results of these measurements were compared to a combined theory incorporating the de Gennes–Werthamer calculation of the proximity effect in nonmagnetic materials^{3–5} and the Abrikosov-Gor'kov model of superconductivity in dilute magnetic alloys.⁶

For a ferromagnetic layer sandwiched between superconducting layers it is expected that the critical temperature T_c decreases monotonically with increasing magnetic layer thickness. Interest in this problem increased considerably, after Wong *et al.*⁷ reported a nonmonotonic dependence of T_c as a function of the Fe thickness in V/Fe superlattices at fixed V thickness. Shortly afterwards the possibility of an oscillation of T_c as a function of the ferromagnetic layer thickness in SC/FM multilayers was demonstrated

theoretically.⁸ It was shown that for specific ferromagnetic layer thicknesses the Josephson coupling between two superconducting layers can lead to a junction with an intrinsic phase difference $\Delta\phi = \pi$ which, in turn, exhibits a higher T_c value compared to the ordinary phase difference $\Delta\phi = 0$. Such so-called π junctions have been suggested earlier to arise also in tunnel barriers, containing magnetic impurities⁹ and have been proposed recently for weak links of superconductors with d -wave pairing.¹⁰ Although numerous experimental results were discussed in terms of π junctions, unequivocal observations of π -junction coupling involving conventional superconductors has not been published yet.

The evidence for π coupling in SC/FM multilayers was sought experimentally in V/Fe,¹¹ Nb/Gd,^{12,13} and Nb/Fe (Ref. 14) systems.¹⁵ In V/Fe,¹¹ contrary to the previous results,⁷ T_c oscillations as a function of d_{Fe} were not observed. Negative results were also published for the Nb/Fe system.¹⁴ At the same time, for Nb/Gd a nonmonotonic dependence of T_c on d_{Gd} for fixed d_{Nb} was reported by Strunk *et al.*,¹² and by Jiang *et al.*¹³ For the explanation of the nonmonotonic T_c behavior two different qualitative explanations were proposed. Strunk *et al.* assumed that the obtained T_c behavior could be attributed to the change in the underlying pair-breaking mechanism at the transition of the Gd layer from the paramagnetic to the ferromagnetic state with increasing d_{Gd} . In contrast, Jiang *et al.* suggested that the oscillatory T_c behavior provides evidence for the predicted π -phase differences in SC/FM multilayers.

In order to test the validity of these ideas we prepared Fe/Nb/Fe-trilayer samples consisting of one single supercon-

ducting layer between two Fe layers. Nevertheless, a non-monotonic $T_c(d_{\text{Fe}})$ at fixed d_{Nb} looking very similar to the $T_c(d_{\text{Gd}})$ in Nb/Gd multilayers reported by Jiang *et al.*¹³ was observed. Contrary to their interpretation we conclude that the nonmonotonic $T_c(d_{\text{Fe}})$ occurs due to the existence of magnetically “dead” Fe layers near the interface and their properties changing drastically upon the onset of ferromagnetic order.¹⁶

The paper is organized as follows: Secs. II and III provide a brief outline of the sample preparation and characterization. Results of the study of magnetic properties using the magneto-optical Kerr effect (MOKE), ferromagnetic resonance (FMR), and superconducting quantum interference device (SQUID) magnetometer are presented in Sec. IV. Results of the measurements of the superconducting parameters when varying the Fe and Nb thickness are provided in Sec. V. In Sec. VI the results in terms of different pair-breaking effects are discussed. Finally the main results are summarized in Sec. VII.

II. FILM PREPARATION

We have prepared the Fe/Nb/Fe trilayers by rf sputtering on high-quality Al_2O_3 (11 $\bar{2}$ 0) substrates at room temperature using very pure Nb (99.99%) and Fe (99.99%) targets. Pure Ar (99.99%) at pressures of 5×10^{-3} mbar has been used as a sputter gas. The base pressure was 8×10^{-8} mbar after cooling with liquid N_2 . Prior to deposition the substrates were ultrasonically cleaned in acetone and then in ethanol for 15 min, respectively. Subsequently they were annealed for 6 h at 770 K and plasma etched with 150-eV Ar ions. The growth rate was controlled by a quartz crystal monitor and a rate of 0.1 Å/sec was found to be optimal for the quality of the films. The film thicknesses were finally confirmed by *ex situ* x-ray-reflectivity measurements.

In order to find the optimal growth conditions for the Fe/Nb/Fe trilayers, we performed systematic resistivity measurements on single Nb films deposited under different conditions. The T_c value and the residual resistivity $\rho(10 \text{ K})$ are extremely sensitive to the preparation conditions. In fact, we find that T_c depends on the time between igniting the plasma and starting the film deposition. We suppose that the higher values for T_c of the samples prepared later from the starting moment of the deposition result from a purification of the target surface during the evaporation process. Our measurements of the residual resistance ratio $\text{RRR} = R_{300 \text{ K}}/R_{10 \text{ K}}$ shows that there is a close correlation between T_c and RRR in accordance with the results obtained by Sürgers *et al.*,¹⁷ and by Park *et al.*,¹⁸ for samples prepared by molecular beam epitaxy (MBE). We observed that with increasing d_{Nb} the value of $\rho(10 \text{ K})$ decreases monotonically, indicating that the conduction electron scattering at grain boundaries is the main scattering process. Usually in thin films (see, e.g., Ref. 12 and references therein) the mean grain size scales with the film thickness. With decreasing RRR the superconducting transition temperature decreases monotonically. This dependence of T_c on the rate of conduction electron scattering is caused by the so-called lifetime “broadening” of the electronic density of states.¹⁹ Conduction electron scattering leads to a decrease of the density of states at the Fermi level and is especially important for transition metals with a nar-

TABLE I. Summarized parameters for all Fe/Nb/Fe trilayer systems used for the present investigation. First column: sample series number used throughout the text. Second column: nominal thickness of the Nb layer. Third column: nominal Fe thickness and magnetic state of the Fe layers.

Sample series	d_{Nb} (Å)	d_{Fe} (Å)	
		Nonmagnetic	Magnetic
S502	400	0	
	400	4	
	400	7	
	400		10
	400		13
	400		16
	400		19
	400		22
S532	400	0	
	400	6	
	400	8	
	400		10
	400		14
	400		25
	400		30
S528	450	0	
	450	5	
	450	7	
	450	8	
	450	9	
	450	10	
	450	12	
S555	300	7	
	320	7	
	340	7	
	360	7	
	400	7	
	500	7	
	600	7	
	700	7	
800	7		
S510	320		16
	340		16
	360		16
	380		16
	400		16
	500		16
	600		16
700		16	
800		16	

row peak in the density of states near the Fermi level. We find a maximum T_c of 7 K for a single Nb films with $d_{\text{Nb}}=400 \text{ Å}$ and $\rho(10 \text{ K}) \approx 13 \mu\Omega \text{ cm}$. Increasing the Nb thickness up to $d_{\text{Nb}}=1500 \text{ Å}$, the value of T_c increases to 8 K and $\rho(10 \text{ K})$ drops to $10 \mu\Omega \text{ cm}$. The residual resistivity value allows an estimation of the electron mean-free path l .

TABLE II. Parameters for the Fe/Nb/Fe trilayer system $s5$, $s15$, $s25$ as derived from the Parratt fit given in Fig. 1 of Ref. 16. d_A denotes the thickness of the layer A in the sequence from the top layer to the bottom layer, σ_A denotes the roughness parameter of layer A (see Fig. 1).

	d_O (Å)	d_{Nb} (Å)	d_{Fe} (Å)	d_{Nb} (Å)	d_{Fe} (Å)	d_{Nb} (Å)	σ_O (Å)	σ_{Nb} (Å)	σ_{Fe} (Å)	σ_{Nb} (Å)	σ_{Fe} (Å)	σ_{Nb} (Å)	$\sigma_{substrate}$ (Å)
$s5$	32	14.3	5.5	101	5.5	29	6.2	2.9	4.1	4.2	3.2	6	4.4
$s15$	27.8	21	16.3	101	16	30	4.3	3.3	3	5	4.1	3.1	2.6
$s25$	23.4	20	24	99	24.3	30	3.6	4.3	3.1	3	2.8	3	3.9

Using the experimental density of states at the Fermi surface and the experimental value of the Fermi velocity for Nb, $\langle \rho l \rangle = 3.75 \times 10^{-6} \mu\Omega \text{ cm}^2$ has been obtained²⁰ in the frame of a ‘‘dressed’’ Drude theory. This gives $l \approx 29 \text{ Å}$ for our single Nb films with $d_{Nb} = 400 \text{ Å}$.

In order to study carefully the dependences of the superconducting parameters on the thickness d_{Fe} (or d_{Nb}), it is essential that the samples are deposited under identical conditions and the relative thicknesses are determined with an accuracy as high as possible. Therefore in our experimental setup series of 7–9 samples with different d_{Fe} at constant d_{Nb} were prepared within one run. Prior to the trilayer growth a Nb layer of 30 Å thickness was deposited on the sapphire substrates as a buffer layer and in order to ensure symmetrical interfaces for the iron layers. After this, for the preparation of a series of triple layers with $d_{Nb} = \text{const}$ and variable d_{Fe} , a shutter was opened for the evaporation of Fe on all substrates, which were arranged in an array. After a certain time (typically 30 sec depending on the deposition rate) the shutter for the first sample was closed, then for the second and so on with an interval of 30 sec between the closing time for each subsequent sample. When the evaporation of Fe was finished, all substrate shutters were opened simultaneously for the evaporation of Nb. Afterwards the process for the evaporation for the top Fe layer was repeated in the same fashion as before. In a final step all samples were covered by a protective Nb cap layer of about 30-Å thickness. The preparation of triple layers with constant d_{Fe} and variable d_{Nb} was achieved in a similar manner.

After choosing the optimal growth conditions, five series of samples with thicknesses d_{Nb} and d_{Fe} as summarized in Table I have been prepared for the present investigation. It should be noted that there were only minor differences between the preparation conditions of the series S502 and S532 and of the series S528 in Table I. In addition, one multilayer sample $[\text{Fe}(7 \text{ Å})/\text{Nb}(30 \text{ Å})]_{20}$ has been prepared specifically for precise magnetization measurements. The sample series S517 (see Table II) with nominal thicknesses $d_{Nb} = 100 \text{ Å}$, $d_{Fe} = 5, 15, \text{ and } 25 \text{ Å}$ was grown on large ($1 \times 1 \text{ cm}^2$) substrates and were intended for detailed x-ray measurements.

III. STRUCTURE AND ROUGHNESS

The structure of the thin-film system of the present study was characterized in detail by low-angle x-ray-reflectivity measurements. Original x-ray spectra revealing well-resolved superstructure and thin-film thickness oscillations (Kiessig fringes) have been given in Fig. 1 of Ref. 16. Thickness and roughness parameters of the layers have been derived using the Parratt formalism.²¹ Table II summarizes the corresponding parameters for the three samples $s5$, $s15$, $s25$

as a representative example for a trilayer system of the present study. It should be noted that the thickness parameters coincide approximately with the values determined by the quartz crystal monitor during deposition ($d_{Nb} = 100 \text{ Å}$, $d_{Fe} = 5, 15, \text{ and } 25 \text{ Å}$). The roughness parameters of 3–4 Å are indicative of the high structural quality of the films. We found that the absolute value of d_{Fe} and d_{Nb} determined by the fit procedure may deviate by up to 10% from the thickness determined by the quartz crystal monitor during deposition. Using the Parratt fit, we also checked the d_{Nb} values within one sample series with changing Fe thickness. In this case the scatter of d_{Nb} was much lower, namely about 1%.

The complex refractive index for x-ray radiation is given by^{22,23}

$$n_1 = 1 - \rho_n(Z + \Delta f') \frac{r_0 \lambda^2}{2\pi} - i \frac{\lambda \mu}{4\pi} = 1 - \delta - i\beta. \quad (1)$$

Here λ is the x-ray wavelength, r_0 the classical electron radius, ρ_n the number of atoms per volume, Z the atomic number, $\Delta f'$ the dispersion correction, and μ the mass absorption coefficient. The normalized parameters δ and β are proportional to the electron density $\rho_n Z$ and to the absorption of x rays, respectively. In the present case the contrast in the reflectivity spectra mainly results from the different absorption of $\text{Mo}_{K\alpha 1}$ radiation in Nb and Fe. This can be seen in Figs. 1(a) and 1(b), where the δ and β profile of the samples with $d_{Fe} = 15 \text{ Å}$ is shown. In Fig. 1(c), the first derivative of the δ profile is presented, showing more clearly the interface region with a width of $\approx 7 \text{ Å}$.

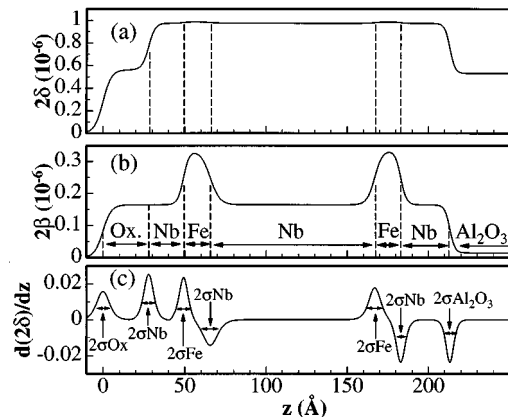


FIG. 1. 2δ and 2β profile of the sample with $d_{Fe} = 15 \text{ Å}$. The lower panel is the first derivative of the 2δ profile showing more clearly the interface region of $\approx 7 \text{ Å}$.

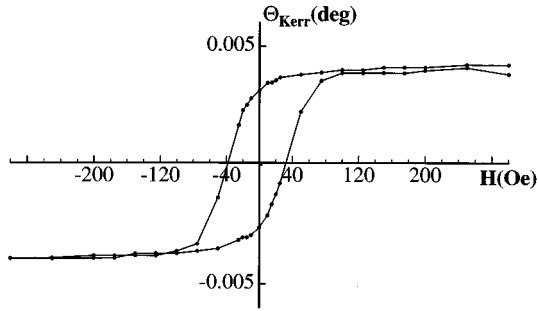


FIG. 2. MOKE hysteresis loop for the sample with $d_{\text{Fe}}=22$ Å from series S502 measured at room temperature.

X-ray Bragg reflection measurements showed that the films are (110)-textured perpendicular to the film plane with a mosaicity of about 2° . Estimates of the grain size give typical values of about 50 Å.

IV. MAGNETIC PROPERTIES

A. Magneto-optical Kerr effect

We have taken longitudinal MOKE measurements at room temperature with a high-resolution modulation technique which is described in detail in Ref. 24. The ferromagnetic MOKE signal in our trilayers could be registered for the samples with $d_{\text{Fe}} \geq 20$ Å only, for films with $d_{\text{Fe}} < 20$ Å no MOKE hysteresis loop could be resolved. The hysteresis loops, an example is shown in Fig. 2, exhibit a coercive force $H_c \approx 40$ Oe and are typical for thin Fe films.

B. Ferromagnetic resonance

FMR measurements for the three series of the samples with varying d_{Fe} (series S502, S532, and S528 from Table I) were carried out at 9.4 GHz in a rectangular TE_{102} cavity of the EPR spectrometer B-ER 418^s (Bruker AG). For the samples from the series S502 and S532 with d_{Fe} decreasing from 25 to 16 Å, a FMR signal was observed with a linewidth $\Delta H_{pp} \sim 160$ Oe, whereas for the samples with $d_{\text{Fe}} \leq 14$ Å the FMR linewidth increased up to $\Delta H_{pp} \approx 500$ Oe. No FMR signal was observed for the samples with $d_{\text{Fe}} \leq 10$ Å. Figure 3 shows the results of $\Delta H_{pp}(d_{\text{Fe}})$ at room temperature

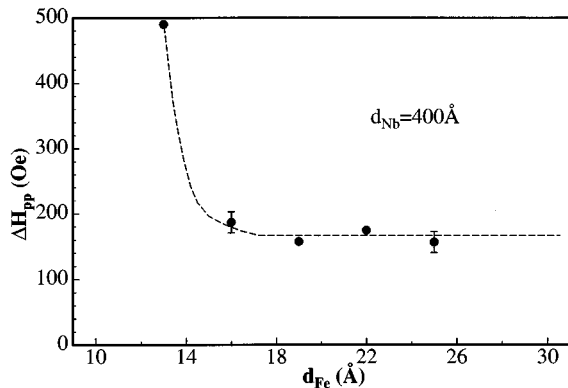


FIG. 3. The thickness dependence of the FMR linewidth for the samples from series S502 measured at room temperature.

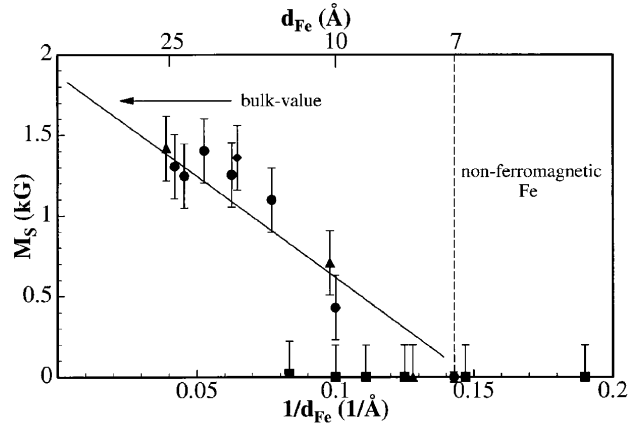


FIG. 4. Saturation magnetization measured by a SQUID magnetometer at $T=10$ K versus $1/d_{\text{Fe}}$ for the samples from series S502 (circles), S532 (triangles), S528 (squares), and S510 ($d_{\text{Nb}}=800$ Å, rhomb). The solid line is a linear fit for series S502 and S532. Note that the measurements for the sample with $d_{\text{Fe}}=7$ Å from series S502 were performed with higher precision.

for the samples from the series S502 as an example. With decreasing temperature the observed FMR signals did not undergo noticeable changes down to 1.7 K. Only a slight, continuous broadening of the resonance line was observed. For all samples from series S528, no FMR signal could be detected.

C. Magnetization

Magnetization measurements using a SQUID magnetometer were performed in the temperature range from 10 to 100 K with the film surface parallel to the direction of the magnetic field. For the two series S502 and S532 these measurements did not indicate any qualitative differences in the magnetization curves when changing d_{Fe} between 10 and 25 Å. The hysteresis loops have the typical square shape, similar to the MOKE hysteresis loops in Fig. 2. For the samples with $d_{\text{Fe}} \leq 8$ Å a contribution to the magnetization from the Fe layers could not be detected for the series S502 and S532, for the series S528 the same holds true for all samples with $d_{\text{Fe}} \leq 12$ Å. The dependence of the saturation magnetization M_s on the reciprocal thickness of the Fe layers is shown in Fig. 4. The main magnetic properties of all samples are also included in Table I.

We have analyzed the magnetic state of the Fe atoms close to the interface by a comparative high-resolution magnetization measurements of a pure Nb film and of the film with $d_{\text{Fe}}=7$ Å (both from the series S502). In the temperature range from 10 to 100 K and in a magnetic field up to 2500 Oe, the magnetization values were equal within the experimental error bars for both samples (Fig. 5). The solid line shows the expected paramagnetic contribution according to the Curie law in comparison. The absence of any contribution to the magnetization from the 7-Å-thick Fe layers has also been confirmed by our SQUID measurements of a specifically prepared multilayered sample $[\text{Nb}(30 \text{ Å})/\text{Fe}(7 \text{ Å})]_{20}$.

It is necessary to note that the paramagnetic contribution to the magnetic moment of the samples caused by uncontrolled impurities in the substrate material becomes predominant at low temperatures. In order to correct this contribution of the substrate, $M(H)$ measurements were performed up to

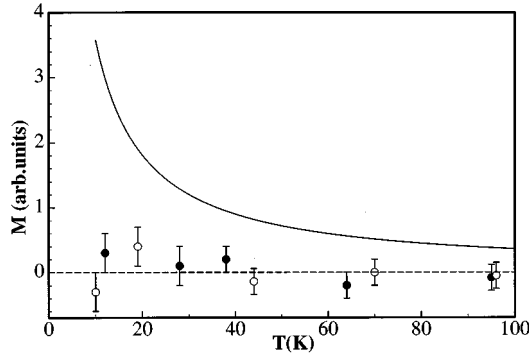


FIG. 5. Magnetization measured by a SQUID magnetometer in a magnetic field of 2500 Oe for the samples from series S502 with $d_{\text{Fe}}=0$ (open circles) and with $d_{\text{Fe}}=7$ Å (solid circles). The solid line shows the expected magnetization behavior for Fe in the 7-Å-thick layer in the paramagnetic state (Curie law).

the saturation magnetization at each temperature. The contribution of the substrate, linearly depending on the magnetic field, was subtracted from the measured $M(H)$ curve, giving the value defined as M_S for the Fe layers in Fig. 4. For the samples without ferromagnetic contributions the magnetic moment of the substrates was also measured separately after removing the metallic layers. For our substrates at room temperature we observed a diamagnetic behavior. With decreasing temperature the magnetic susceptibility of the substrates crosses zero at about 40 K and then increases strongly. This is the reason for the increasing error bars in Fig. 5 at low temperatures.

V. SUPERCONDUCTING PROPERTIES

The superconducting transition temperature T_c and upper critical field $H_{c2}(T)$ for parallel [$H_{c2\parallel}(T)$] and perpendicular [$H_{c2\perp}(T)$] orientations of the magnetic field relative to the film plane were measured resistively in a standard four-terminal configuration and defined as the midpoint of the superconducting transition. The current and voltage leads were attached to the samples with silver paint. $H_{c2}(T)$ was measured by sweeping the magnetic field at constant temperature. In addition, ac magnetic susceptibility measurements were used to determine T_c for all samples. In this case the temperature corresponding to half the value of the maximum transition signal was defined as T_c . The superconducting transitions for four samples of series S502 have been shown in Fig. 3 of Ref. 16 and are very sharp thus confirming the high quality of our trilayer films.

A. Critical temperature

The T_c dependence on d_{Fe} obtained for the two series of trilayers S502 and S532 with fixed $d_{\text{Nb}}=400$ Å is shown in Fig. 6(a). A strong initial T_c depression is observed up to $d_{\text{Fe}}=7$ Å. For larger d_{Fe} the value of T_c increases markedly reaching a maximum at $d_{\text{Fe}}=10-12$ Å and then decreases with a tendency to saturation for $d_{\text{Fe}}\geq 20$ Å. It should be emphasized that the maximum in T_c at $d_{\text{Fe}}=10-12$ Å in Fig. 6(a) is outside of any possible experimental error.

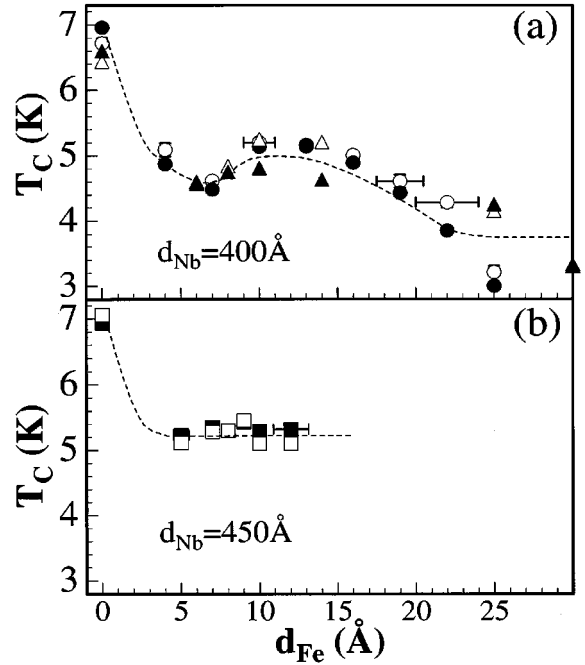


FIG. 6. Superconducting transition temperature T_c as a function of d_{Fe} as determined by ac susceptibility (solid symbols) and resistivity (open symbols) measurements. The triangles, circles, and squares correspond to series S502, S532, and S528, respectively. The dashed lines are guide for the eyes.

In Fig. 6(b), the $T_c(d_{\text{Fe}})$ dependence for the samples from series S528 is presented for comparison. As discussed above, in this series no indication of ferromagnetic ordering is observed for $d_{\text{Fe}}\leq 12$ Å. Remarkably, similar to the case of our previous series S502 and S532, at small iron thicknesses ($d_{\text{Fe}}<5$ Å) a strong initial T_c depression is observed. However, the T_c value saturates at $T_c\approx 5.3$ K and develops no maximum up to the highest $d_{\text{Fe}}=12$ Å prepared within this series.

The dependence of $T_c(d_{\text{Nb}})$ obtained for two series of samples with fixed $d_{\text{Fe}}=7$ Å (S555) and $d_{\text{Fe}}=16$ Å (S510)

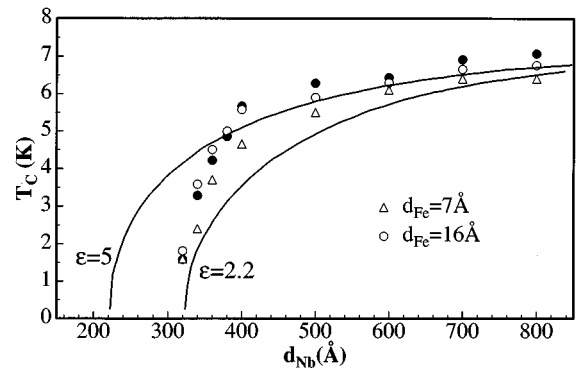


FIG. 7. Superconducting transition temperature T_c as a function of d_{Nb} as determined by ac susceptibility (solid symbols) and resistivity (open symbols) measurements for samples from series S555 and S510 with fixed d_{Fe} . The triangles and circles correspond to two different Fe thicknesses $d_{\text{Fe}}=7$ and 16 Å, respectively. The solid lines are theoretical curves with the parameter $\varepsilon=5$ and $\varepsilon=2.2$ and taking $T_{c0}=7.5$ K (see main text and Ref. 25).

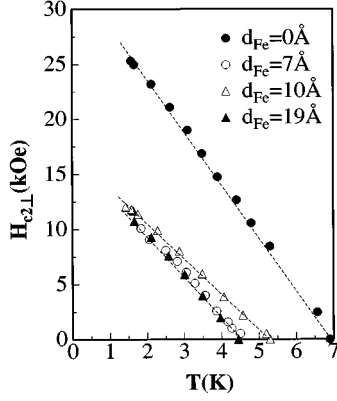


FIG. 8. The perpendicular upper critical field $H_{c2\perp}$ vs temperature for samples from series S502 with fixed $d_{\text{Nb}}=400$ Å and different values of d_{Fe} .

is shown in Fig. 7. The T_c value decreases slightly when decreasing the Nb thickness from $d_{\text{Nb}}=800$ Å down to $d_{\text{Nb}}\approx 400$ Å and then starts to decrease sharply down to a critical thickness $d_{\text{Nb}}^{\text{crit}}$ below which the superconductivity vanishes. We extrapolate $d_{\text{Nb}}^{\text{crit}}\approx 320$ Å for both series. It should be mentioned that if one reads the value of T_c at $d_{\text{Fe}}=7$ and 16 Å from Figs. 6(a) and 6(b) and presents them in Fig. 7, one would obtain some difference between these points and the $T_c(d_{\text{Nb}})$ curve. However, one should bear in mind that the error bars for the absolute value of the Nb thickness are about 10%, which makes a direct comparison of results obtained on different sample series difficult. On the other hand, the experimentally determined thicknesses of the Nb layers for the series S502 with $d_{\text{Nb}}=400$ Å are known within an error bar of 1% for all samples. We stress once more that within one series of samples the Nb layer is evaporated simultaneously from the same source, thus the scattering of d_{Nb} is very low. This implies that we can control the thickness d_{Nb} within one series to about ± 4 Å, and from the results given in Fig. 7 we then can conclude that this is by far enough to exclude the variation of d_{Nb} as responsible for the oscillations of T_c shown in Fig. 6(a).

B. Critical fields

We performed measurements of the anisotropic upper critical fields $H_{c2\parallel}(T)$ and $H_{c2\perp}(T)$ for selected samples from series S502. The Fe thickness for these samples corresponds to some special points along the $T_c(d_{\text{Fe}})$ curve in Fig. 6(a): i.e., starting $T_c(d_{\text{Fe}}=0)$, minimum $T_c(d_{\text{Fe}}=7$ Å), maximum $T_c(d_{\text{Fe}}=10$ Å), and finally decreasing $T_c(d_{\text{Fe}}=19$ Å) just before saturation.

The measurements with the magnetic field perpendicular to the surface of the film ($H_{c2\perp}$) (Fig. 8) show a linear temperature dependence near T_c :

$$H_{c2\perp}(T) = H_{c2\perp}(0)(1 - T/T_c). \quad (2)$$

We obtain the values of $H_{c2\perp}(0)=35$ kOe for the single Nb film and $H_{c2\perp}(0)=17.5$ kOe for the trilayer samples. In the framework of the Ginzburg-Landau theory $H_{c2\perp}$ for a superconducting film is given by $H_{c2\perp}(0)=\phi_0/2\pi\xi^2(0)$ with ϕ_0 being the flux quantum and ξ the in-plane coherence

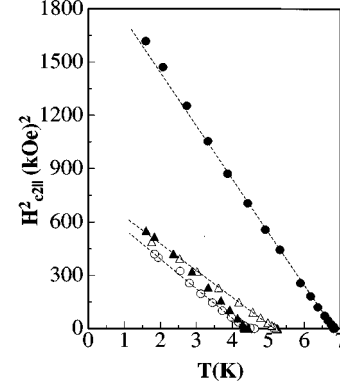


FIG. 9. Square of the parallel upper critical field $H_{c2\parallel}$ vs temperature for the same samples as in Fig. 8.

length. The extrapolation in Fig. 8 yields a coherence length $\xi(0)\approx 95$ Å for a single Nb film. The superconducting coherence length ξ_S in Refs. 8 and 25 is related to the Ginzburg-Landau coherence length $\xi(T)$ via

$$\xi(T) = \frac{\pi}{2} \xi_S (1 - T/T_c)^{-1/2}. \quad (3)$$

This gives $\xi_S\approx 60$ Å. The value of ξ_S can also be estimated from²⁵

$$\xi_S = \sqrt{\frac{\hbar D_S}{2\pi k_B T_{cS}}} = \sqrt{\frac{\xi_{\text{BCS}} l}{3.4}}, \quad (4)$$

where $D_S=(1/3)v_F l$ is the diffusion coefficient in the superconducting metal, v_F the Fermi velocity, $\xi_{\text{BCS}}=0.18\hbar v_F/k_B T_{cS}$ the BCS coherence length, and T_{cS} the value of T_c for a single superconducting film. Using $v_F=2.77\times 10^7$ cm/s,²⁰ $T_{cS}=7$ K and the value for the mean free path $l=29$ Å as determined from the residual resistivity above for our single Nb films with $d_{\text{Nb}}=400$ Å, we estimate $\xi_S=68$ Å which is only slightly larger than the ξ_S value determined from $H_{c2\perp}(0)$.

The behavior of the upper critical field with the field parallel to the film surface $H_{c2\parallel}$ (Fig. 9) can well be described by the formula for a two-dimensional superconductor:

$$H_{c2\parallel}(T) = H_{c2\parallel}(0)(1 - T/T_c)^{1/2}. \quad (5)$$

From a fit to the data points we find the values of $H_{c2\parallel}(0)=45$ kOe for the single Nb film and $H_{c2\parallel}(0)=28.6$ kOe for trilayered samples.

VI. DISCUSSION

A. Magnetic properties

The analysis of the experimental data shows that the disappearance of the magneto-optical Kerr effect signal for the samples with $d_{\text{Fe}}<20$ Å is due to the limited sensitivity of our equipment. The strong broadening of the FMR signal for the sample with $d_{\text{Fe}}\leq 13$ Å from series S502 and S532 and its disappearance for the samples with $d_{\text{Fe}}=10$ Å is probably due to inhomogeneities in the magnetization caused by alloying effects near the interface.

Figure 4 reveals a decrease of the saturation magnetization M_s with decreasing d_{Fe} . There are two possible explanations for this dependence. First, the reduction of M_s could be due to a lowering of the atomic magnetic moment of Fe in our Fe/Nb/Fe trilayers, e.g., due to alloying of the whole Fe layer with Nb. In this case, however, we should expect a continuous FMR line broadening with decreasing d_{Fe} , due to the dispersion of the internal magnetic field in ferromagnetic alloys. In Fig. 3, however one notices that the broadening of the FMR line sets in at $d_{\text{Fe}}=13$ Å only, showing that for series S502 the alloying effect is only important for the samples with $d_{\text{Nb}} \leq 13$ Å. This broadening of the FMR line is probably also the reason for the disappearance of the resonance signal in the ferromagnetic sample with $d_{\text{Fe}}=10$ Å.

We believe that the reduction of the saturation magnetization in Fig. 4 is due to the existence of a magnetically “dead” Fe-rich, nonmagnetic layer, formed by alloying at the interface. In Nb/Fe superlattices this effect was observed previously by Mattson *et al.*²⁶ in their measurements of the saturation magnetization. They observed that about 7 Å of each Fe layer is not ferromagnetic and hence not contributing to the magnetization. It seems conceivable that the average concentration of Fe in this magnetically “dead” layer is of the order of 50 at %. Mössbauer results by Chien *et al.*²⁷ show that Nb-Fe alloys with 50 at % Fe are close to the transition point from nonmagnetic to ferromagnetic alloys (≈ 60 at % Fe). Recently Luo and Krebs²⁸ have reported on the formation of amorphous or strongly disordered crystalline interlayers of 2.5 Å thickness in the interface region between the Fe and Nb crystalline layers by x-ray-diffraction studies. The multilayers were sputtered at room temperature with preparation conditions very similar to ours. Hence we can imagine that at each Fe/Nb interface a nonmagnetic Fe/Nb alloy is formed with an amorphous or strongly disordered crystalline state in the middle. The thickness of this nonmagnetic layer, although being well defined within one sample series, can vary definitely from one series to the other (see Fig. 4), in spite of the fact that we try to keep the experimental parameters during the layer growth identical. We think that the microstructure and concentration gradient at the interface depends very sensitively on the parameters of the discharge, which we can only control within certain limits.

B. Superconducting properties for large Fe thicknesses

A theoretical model for the interpretation of experimental studies of FM/SC multilayers is provided by the microscopic theory by Radović *et al.*^{8,25,29} Among other details, this theory (see Ref. 25) calculates T_c and $H_{c2}(T)$ of a single superconducting film embedded in a ferromagnetic metal. It is assumed that both superconducting and ferromagnetic metals can be described in the dirty limit. Assuming that for the ferromagnetic metal the dominant effect is the polarization of the conduction electrons by the strong exchange field and neglecting other possible depairing mechanisms in the superconductor, the authors calculate T_c as a function of the reduced superconducting film thickness d_S/ξ_S and $H_{c2}(T)$ for parallel and perpendicular orientations of the magnetic field. In this theory the parameter $\varepsilon = \xi_M/\eta\xi_S$ is essential. ε denotes the proximity effect parameter and is determined by the superconducting coherence length ξ_S , the characteristic

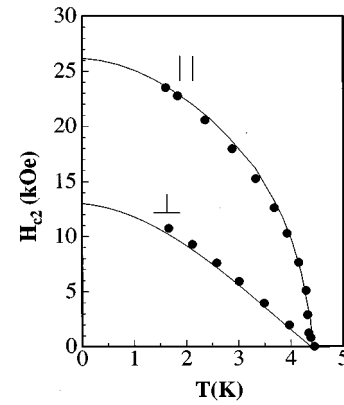


FIG. 10. The upper critical field $H_{c2\perp}$ and $H_{c2\parallel}$ vs temperature for the sample from series S502 with $d_{\text{Nb}}=400$ Å and with $d_{\text{Fe}}=19$ Å. Solid lines present fits according to the theory of Ref. 25.

distance of the decay of the pair wave function in the ferromagnet $\xi_M = \sqrt{4\hbar D_M/I}$, and the parameter η characterizing the interface transparency (D_M is the diffusion coefficient in the ferromagnet, and I is the exchange field polarizing the conduction electrons).

Our measurements of the $T_c(d_{\text{Nb}})$ at fixed d_{Fe} (Fig. 7) show that the superconductivity vanishes at a critical thickness $d_{\text{Nb}}^{\text{crit}} \approx 320$ Å. Bearing in mind that for our samples $\xi_S \approx 68$ Å, we obtain the reduced critical film thickness $d_S/\xi_S = 4.7$. According to the theory²⁵ this corresponds to $\varepsilon \approx 2.2$. Fitting our results in Fig. 7 by using this parameter and $T_{cS} = 7.5$ K shows bad agreement (see Fig. 7). Another possibility to determine the parameters of the theory is by fitting the theoretical curve from Ref. 25 to the data on $H_{c2}(T)$ in Fig. 10. The best fit for the sample with $d_{\text{Fe}} = 19$ Å shown by solid lines in Fig. 10 corresponds to $\varepsilon = 5$. Fitting $T(d_{\text{Nb}})$ dependence by using this ε value shows good agreement at large Nb thickness but a theoretical value for the critical thickness $d_{\text{Nb}}^{\text{crit}}$ much smaller than the one observed experimentally (see Fig. 7).

The above analysis shows that our experimental results cannot be described quantitatively in the framework of the theory by Radović *et al.*, probably because of the existence of a magnetically dead layer in our samples which is a more complex situation than assumed in the theoretical model. Indeed, our results on the $T_c(d_{\text{Nb}})$ for the series S555 and S510 at two fixed d_{Fe} (Fig. 7) show that there is no difference in $T_c(d_{\text{Nb}})$ for the series with the non-magnetic Fe layer ($d_{\text{Fe}}=7$ Å, series S555) and with the ferromagnetic Fe layers ($d_{\text{Fe}}=16$ Å, series S510). Similarly, in Figs. 8 and 9 there is essentially no difference between $H_{c2}(T)$ for the samples from series S502 with $d_{\text{Fe}}=7$ Å (nonmagnetic Fe layer) and with $d_{\text{Fe}}=19$ Å (ferromagnetic Fe layer). The minute difference for the $H_{c2\parallel}(T)$ curves is rather caused by the uncertainty in the angle between the film plane and orientation of magnetic field, because close to the parallel orientation the angular dependence of H_{c2} is much stronger than in the perpendicular orientation.

C. Dependence of the superconducting transition temperature on the Fe thickness

The most important result in our present study is the existence of a pronounced maximum in $T_c(d_{\text{Fe}})$ at $d_{\text{Fe}} \approx 10$ Å in

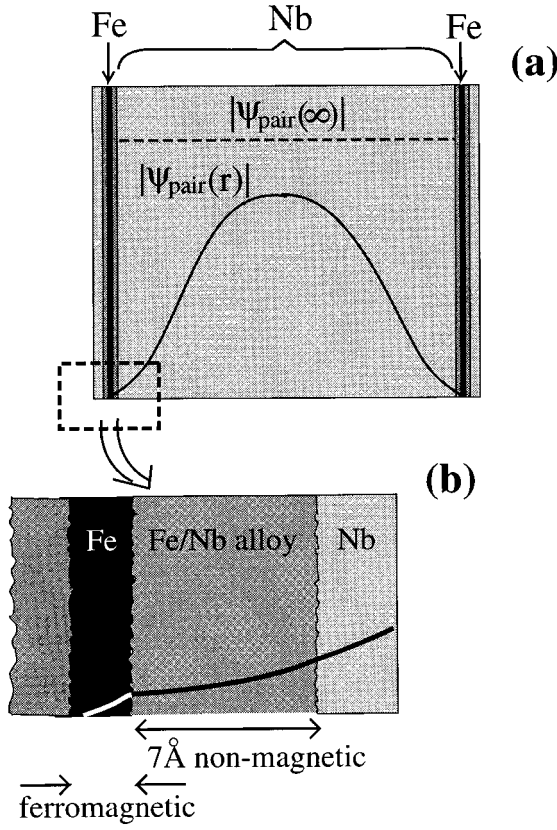


FIG. 11. Schematic picture of the superconducting wave function amplitude in the trilayer system (a). (b) shows the interface region in more detail.

Fig. 6(a) for the series S502 and S532 and its absence for the series S528 in Fig. 6(b). As we mentioned in the Introduction, Jiang *et al.*,¹³ obtained a maximum in $T_c(d_{\text{Fe}})$ very similar to ours and interpreted it as an evidence for π coupling in SC/FM multilayers.⁸ In principal, one could assume that the coupling of the main superconducting Nb layer of our trilayer system with the very thin Nb cap and buffer layers might give rise to a π -coupling effect, too. However, we would rule out this explanation for the following reasons.

First, we note that the difference in the free energy as well as in T_c between a conventional and a π -phase contact of two superconducting layers SC(1)/FM/SC(2) must vanish as d_1/d_2 in the limit $d_1 \gg d_2$ [here d_1 and d_2 denote the thicknesses of the SC(1) and SC(2)]. For our samples the ratio d_1/d_2 is of the order of 0.1. This makes the π -junction effect irrelevant in our case, even if assuming a difference between maximum and minimum in $T_c(d_{\text{Fe}})$ caused by π coupling of the order of 1 K for a symmetrical contact with $d_1 = d_2$. In addition, the amplitude of the order parameter in the top and bottom layers is expected to be strongly reduced by the lifetime broadening effect in thin Nb layers. We have checked experimentally that single Nb layers with $d_{\text{Nb}} = 30 \text{ \AA}$ are not superconducting above 1.7 K when covered by an Fe layer with $d_{\text{Fe}} \geq 5 \text{ \AA}$.

Our results in Fig. 6(a) suggest that the maximum in T_c is correlated with the onset of ferromagnetism for $d_{\text{Fe}} > 8 \text{ \AA}$ in the series S502 and S532. We have shown in Fig. 4 that ferromagnetism vanishes at $d_{\text{Fe}} < 7 \text{ \AA}$ in our Fe/Nb/Fe trilayers for series S502 and S532 whereas for series S528 it van-

ishes already for $d_{\text{Fe}} \leq 12 \text{ \AA}$. Similarly, for the Nb/Gd system ferromagnetism vanishes for $d_{\text{Gd}} \leq 12 \text{ \AA}$.^{12,13} As discussed above, this occurs probably due to an alloying effect near the interface. In principal, the magnetic atoms in the alloyed interface region may either be in the paramagnetic or in the nonmagnetic state. As will be described below, in either case the observed nonmonotonic $T_c(d)$ behavior can be explained.

From our FMR and magnetization data we visualize the internal structure and the amplitude of the superconducting wave function in our samples as shown schematically in Fig. 11. We have a magnetically dead intermixed Nb-Fe interface layer which is in direct contact with the main superconducting Nb layer from one side and with the ferromagnetic Fe layer from the other side. For the sample with $d_{\text{Fe}} = 7 \text{ \AA}$, the ferromagnetic layer is absent and we have from both sides of the main superconducting Nb layer magnetically dead Fe-rich layers with a total thickness of the order of 14 \AA . How can such a thin magnetically dead layer so effectively suppress superconductivity? A conventional Abrikosov-Gor'kov mechanism of pair-breaking scattering is not effective, since there is no indication for the existence of ordinary local Fe moments with Curie-like behavior (see Fig. 5).

Instead, we can consider Fe-derived d states in the interface region in terms of Friedel-Anderson virtual states or in terms of a Kondo impurities with a large Kondo energy. Although these local virtual states are not usual pair breakers, since their contribution to the elastic spin scattering is small, they strongly suppress superconductivity by inducing repulsive interactions between the conduction electrons. The scale for this local paramagnon mediated repulsion can be roughly estimated as

$$V_{\text{sf}} \approx -n \frac{I_{\text{sd}}^2}{\omega_{\text{sf}}}, \quad (6)$$

where n is the density of Fe ions in the intermixed region, I_{sd} is the exchange coupling constant of the conduction electrons with the d -spin density of the resonant levels, and ω_{sf} is the characteristic energy scale of the local spin fluctuations (the sign of the interelectronic interaction constant is chosen to be positive for attraction). Very roughly, the value of V_{sf} can be estimated from the following considerations. As follows from Fig. 7, the initial thickness of the Nb layer at which superconductivity vanishes for the set of samples with $d_{\text{Fe}} = 7 \text{ \AA}$ is $d_{\text{Nb}}^{\text{crit}} \approx 320 \text{ \AA}$. Using the Cooper limit⁵ for the sake of simplicity we conclude that the effective BCS coupling constant for this $d_{\text{Nb}}^{\text{crit}}$ must vanish:

$$\lambda_{\text{eff}} = \frac{d_1 N_1^2 V_1 + 2d_2 N_2^2 V_2}{d_1 N_1 + 2d_2 N_2} = 0. \quad (7)$$

Here the subscripts 1 and 2 refer to the Nb superconducting film and magnetically dead Fe-Nb intermixed layer, respectively, N_i is the electronic density of states at the Fermi level, V_i is the electron-electron interaction constant, d_i is the layer thickness. λ_{eff} plays the role of an “effective NV ” in the BCS formula for T_c .

$$\ln \frac{1.14 \omega_D}{T_c} = \frac{1}{\lambda_{\text{eff}}} \quad (8)$$

with ω_D being the Debye temperature. Assuming $N_1 \sim N_2$ and keeping in the mind that the real thickness of intermixed layer could be about 14 Å for a nominal thickness of $d_{\text{Fe}} = 7$ Å, we calculated from Eq. 6: $V_2 \approx -V_1 d_1 / 2d_2 \sim -10V_1$. Using for pure Nb the value $V_1 = 0.08$ eV one finds a strongly repulsive interaction $V_2 \sim -1$ eV between electrons in the Fe-Nb interface layer. The existence of such a strong repulsion in an intermixed region will strongly reduce the density of the Cooper pairs, $|\psi_{\text{pair}}(\mathbf{r})| = \langle \psi_i(\mathbf{r}) \psi_l(\mathbf{r}) \rangle$ at the interface (see Fig. 11) ($|\psi_{\text{pair}}(\mathbf{r})|$ is the probability amplitude of finding two electrons in the paired state at point \mathbf{r}). This repulsion originates from spin-fluctuation mediated contribution [Eq. (6)]. Indeed, assuming $n \sim 0.5$ and $I_{\text{sd}} \sim 0.5 - 1$ eV for the local exchange coupling constant one finds that V_{sf} has the value of the order of -1 eV for $\omega_{\text{sf}} \sim 0.1 - 0.5$ eV. Such a scale of spin-fluctuation energy ω_{sf} for Fe ions is plausible.

Ferromagnetism appears first for the series S502 and S532 at $d_{\text{Fe}} = 10$ Å. The observation of the T_c enhancement just at this thickness seems to be highly surprising at first glance, since one would expect an additional suppression of the superconductivity by the internal exchange field of the ferromagnetic layer acting on the Cooper pairs. However, the solution of this apparent paradox can be given within our model proposed above in a very natural way.

The appearance of the ferromagnetic Fe layer induces a Zeeman splitting of the Fe-derived resonant d levels in an intermixed Fe-Nb region. Concomitantly local spin fluctuations in the intermixed layer become strongly suppressed. Formally, the Zeeman splitting of d levels ΔE_z enters in the spin fluctuation contribution V_{sf} via the renormalization of the denominator in Eq. (6), $\omega_{\text{sf}} \rightarrow \omega_{\text{sf}} + \Delta E_z$, hence reducing this contribution. Thus the repulsion between the electrons also decreases, causing an increase of T_c .

Concerning the pair-breaking effect of the ferromagnetic layer on the Cooper pairs, it is actually strongly suppressed due to the presence of the magnetically dead layers between the superconducting Nb and the ferromagnetic Fe layers (see Fig. 11). Strongly repulsive interactions within the intermixed regions make the superconducting wave-function amplitude $|\psi_{\text{pair}}(\mathbf{r})|$ very small at the interface, thus renormalizing the pair-breaking parameter by the small factor $\alpha = |\psi_{\text{pair}}(\text{interface})| / |\psi_{\text{pair}}(\infty)|$. In other words, the dead layers separate superconducting and ferromagnetic layers in real space thus reducing the destructive effect for the Cooper pairs from the ferromagnet. Indeed, without this ‘‘screening’’ effect by the intermixed layer, the pair breaking parameter $\rho \sim I(d_{\text{erro}}/d_{\text{Nb}})$ would be very large, of the order of $10^{-2} I \sim 100$ K assuming an internal exchange field in the Fe layer $I \sim 1$ eV. Therefore, the real value of ρ must be strongly reduced, by a factor $10^{-2} - 10^{-3}$, which originates in our model from the strong reduction of the superconducting condensate density $|\psi_{\text{pair}}(\mathbf{r})|$ at the interface. This model also explains the absence of any difference between $T_c(d_{\text{Nb}})$ for the nonmagnetic and the ferromagnetic series shown in Fig. 7 and the absence of any difference in $H_{c2}(T)$ for nonmagnetic and ferromagnetic samples (see Figs. 8 and 9), since the main influence on the superconductivity comes from the magnetically dead layer.

The local maximum in $T_c(d_{\text{Fe}})$ [Fig. 6(a)] results from the competition of two different effects of the ferromagnetic layer on the superconductivity. The suppression of spin fluc-

tuations in the intermixed region by magnetic exchange field first increases T_c , at larger thicknesses the pair-breaking effect of the ferromagnetic layer dominates and T_c decreases again. This scenario is supported by the $T_c(d_{\text{Fe}})$ curve for the samples from serie S528, i.e., for the series without ferromagnetic layers [see Fig. 6(b)]. For this series only an initial depression of T_c without a maximum is observed, since in this case there is only the suppression of T_c by the repulsive interaction in the interface region.

It is worth stressing that in our model the T_c suppression is dominated by a renormalization of the interactions between electrons (‘‘pair weakening’’ effect) within magnetically dead layers. This effect is qualitatively different from pair breaking by the internal field in a ferromagnetic layer. It is not surprising, therefore, that our data cannot be fully described within the framework of a pair-breaking based theory as worked out by Radović *et al.*^{8,25,29}

We finally note that our model with some modifications can also provide a reasonable explanation of the nonmonotonic T_c behavior observed in the Nb/Gd multilayer system.¹³ Different from the situation in the Nb/Fe system, the Gd ions in the intermixed region have well-defined local spins due to the stability of the $4f$ -magnetic moments. They will give rise to a strong initial T_c depression with increasing d_{Gd} due to the proximity with the Nb side of the sandwich (analogous to the Abrikosov-Gor’kov mechanism of pair-breaking scattering in dilute magnetic alloys⁶). The appearance of a ferromagnetic Gd layer in the middle of the intermixed layer for $d_{\text{Gd}} \geq 12$ Å, will lead to an induced magnetic ordering of the whole intermixed region by the oscillatory RKKY coupling between the Gd spins. One first would assume a sharp drop in $T_c(d_{\text{Gd}})$ when the spins start to order. This effect is usually observed in dilute magnetic alloys where the T_c versus concentration curve often falls off sharply to zero at the appearance of long-range magnetic order. However, sometimes the situation even in rare-earth-based alloy systems is different. Finnemore *et al.*³⁰ found that in $\text{La}_{1-x}\text{Er}_x$ the T_c values are higher than those predicted by the Abrikosov-Gor’kov theory⁶ near the critical concentration. A similar effect was observed by Guertin and Parks³¹ in the alloy $\text{Th}_{1-x}\text{Er}_x$.

In order to understand the maximum in T_c in the rare-earth alloy systems and in the Nb/Gd multilayers, one should first note that the magnetic ordering will strongly suppress the low-energy spin fluctuations and reduce the Abrikosov-Gor’kov pair-breaking mechanism. Second, it seems plausible to assume spin-glass-like ordering of the rare-earth ions in the alloy system and in the intermixed region at the interface of the Nb/Gd multilayers due to the frustrated character of RKKY coupling in random systems. In this case a uniform exchange field will be absent in the intermixed region, even in the magnetically ordered state and an increase of T_c can be expected when freezing out the elastic spin-flip exchange scattering processes by the local exchange field.

VII. SUMMARY

We have studied the magnetic and superconducting properties of FM/SC/FM trilayer systems using Fe/Nb/Fe as an example. We conclude from our results that the oscillatory $T_c(d_{\text{Fe}})$ curve observed by Jiang *et al.*,¹³ cannot be taken

unambiguously as an evidence for the existence of a π phase of superconductivity.⁸ We provided experimental evidence that in Fe/Nb/Fe trilayers the nonmonotonic behavior in $T_c(d_{\text{Fe}})$ occurs due to the existence of a magnetically dead Fe rich layer near the Nb/Fe interface which is in direct contact with the superconducting Nb layer on one side and with the ferromagnetic Fe layer (at $d_{\text{Fe}} \geq 10 \text{ \AA}$) on the other side. We argue that the effective electron-electron interaction in this layer is strongly repulsive and stems from the coupling of the conduction electrons to the local paramagnon fluctuations. This gives rise to a strong initial T_c depression with increasing d_{Fe} up to $d_{\text{Fe}} \approx 7 \text{ \AA}$. For larger d_{Fe} the appearance of a ferromagnetic layer within the magnetically dead layer moderates the destructive effect of the Fe ions in the dead layer

on the superconductivity. This effect is caused by the suppression of spin fluctuations by the ferromagnetic exchange field and leads to a slight increase of T_c . When further increasing d_{Fe} the ordinary T_c depression by the exchange field from the ferromagnetic layer becomes the predominant effect and depresses T_c further.

ACKNOWLEDGMENTS

We would like to thank J. Podschwadeck and C. Leschke for technical support. This work was supported by the Deutsche Forschungsgemeinschaft (DFG-ZA161/6-1) and by the Russian Fund for Fundamental Research (Project No. 96-02-16332a), which are gratefully acknowledged.

*Permanent address: Kazan Physicotechnical Institute of Russian Academy of Sciences, 420029 Kazan, Russian Federation.

- ¹Ø. Fisher and M. Peter, in *Magnetism*, edited by G. T. Rado and H. Suhl (Academic, New York, 1973), Vol. Y, p. 327; M. B. Maple and Ø. Fischer, *Superconductivity and Magnetism* (Springer-Verlag, Berlin, 1982).
- ²J. J. Hauser, H. C. Theurer, and N. R. Werthamer, *Phys. Rev.* **142**, 118 (1965).
- ³P. G. de Gennes and E. Guyon, *Phys. Lett.* **3**, 168 (1963).
- ⁴N. R. Werthamer, *Phys. Rev.* **132**, 2440 (1963).
- ⁵P. G. de Gennes, *Rev. Mod. Phys.* **36**, 225 (1964).
- ⁶A. A. Abrikosov and L. P. Gor'kov, *Zh. Eksp. Teor. Fiz.* **39**, 1781 (1960) [*Sov. Phys. JETP* **12**, 1243 (1961)].
- ⁷H. K. Wong, B. Y. Jin, H. Q. Yang, J. B. Ketterson, and J. E. Hillard, *J. Low Temp. Phys.* **63**, 307 (1986).
- ⁸Z. Radović, M. Ledvij, L. Dobrosavljević, A. I. Buzdin, and J. R. Clem, *Phys. Rev. B* **44**, 759 (1991).
- ⁹L. N. Bulaevskii, V. V. Kuzii, and A. A. Sobyenin, *Pis'ma Zh. Exp. Teor. Fiz.* **25**, 314 (1977) [*JETP Lett.* **25**, 290 (1977)].
- ¹⁰M. Siegrist and T. M. Rice, *J. Phys. Soc. Jpn.* **61**, 4283 (1992).
- ¹¹P. Koorevaar, Y. Suzuki, R. Coehoorn, and J. Aarts, *Phys. Rev. B* **49**, 441 (1994).
- ¹²C. Strunk, C. Sürgers, U. Paschen, and H. v. Löhneysen, *Phys. Rev. B* **49**, 4053 (1994).
- ¹³J. S. Jiang, D. Davidović, Daniel H. Reich, and C. L. Chien, *Phys. Rev. Lett.* **74**, 314 (1995).
- ¹⁴G. Verbanck, C. D. Potter, R. Schad, P. Belien, V. V. Moschalkov, and Y. Bruynseraede, *Physica C* **235-240**, 3295 (1994).
- ¹⁵Magnetic and superconducting properties of Fe/Nb multilayered films have been studied earlier in K. Kawaguchi and M. Sohma, *Phys. Rev. B* **46**, 14 722 (1992).
- ¹⁶Th. Mühge, N. N. Garif'yanov, Yu. V. Goryunov, G. G. Khaliulin, L. R. Tagirov, K. Westerholt, I. A. Garifullin, and H. Zabel, *Phys. Rev. Lett.* **77**, 1857 (1996).
- ¹⁷C. Sürgers, C. Strunk, and H. v. Löhneysen, *Thin Solid Films* **239**, 51 (1994).
- ¹⁸S. I. Park and T. H. Geballe, *Physica B* **135**, 108 (1985).
- ¹⁹L. R. Testardi and L. F. Mattheiss, *Phys. Rev. Lett.* **41**, 1612 (1978).
- ²⁰H. W. Weber, E. Seidl, C. Laa, E. Schachinger, M. Prohammer, A. Junod, and D. Eckert, *Phys. Rev. B* **44**, 7585 (1991).
- ²¹L. G. Parratt, *Phys. Rev.* **95**, 359 (1954).
- ²²B. E. Warren, *X-ray Diffraction* (Dover, New York, 1990).
- ²³H. Zabel, *Appl. Phys. A* **58**, 159 (1994).
- ²⁴N. Metoki, Th. Zeidler, A. Stierle, K. Bröhl, and H. Zabel, *J. Magn. Magn. Mater.* **118**, 57, (1993).
- ²⁵Z. Radović, L. Dobrosavljević-Grujić, A. I. Buzdin, and J. R. Clem, *Phys. Rev. B* **38**, 2388 (1988).
- ²⁶J. E. Mattson, C. H. Sovers, A. Berger, and S. D. Bader, *Phys. Rev. Lett.* **68**, 3252 (1992).
- ²⁷C. L. Chien, K. M. Unruh, and S. H. Liou, *J. Appl. Phys.* **53**, 7756 (1982).
- ²⁸Y. Luo and H. U. Krebs, *J. Appl. Phys.* **77**, 1482 (1995).
- ²⁹M. Ledvij, L. Dobrosavljević, Z. Radović, and J. R. Clem, *Phys. Rev. B* **44**, 859 (1991).
- ³⁰D. K. Finnemore, D. C. Hopkins, and P. E. Palmer, *Phys. Rev. Lett.* **15**, 891 (1965).
- ³¹R. P. Guertin and R. D. Parks, *Solid State Commun.* **7**, 59 (1969).